THE ASTROPHYSICAL JOURNAL, 451:784–794, 1995 October 1

DOPPLER IMAGING OF THE COOL SPOT DISTRIBUTION ON THE WEAK T TAURI STAR V410 TAURI

ARTIE P. HATZES
McDonald Observatory, University of Texas at Austin, Austin, TX 78712
Received 1995 January 19; accepted 1995 April 11

ABSTRACT

A Doppler image of the spot distribution of the "naked" T Tauri star V410 Tau in epoch 1994.0 is presented. This image was derived using six photospheric absorption lines, and it shows a spot distribution dominated by a high-latitude spot whose center is offset from the rotation pole of the star and several midlatitude spots. V410 Tau may have a spot morphology similar to that seen in two other young stars (V824 Ara and HDE 283572), but slightly different to that seen in RS CVn stars, which tend to have a polar spot centered on the rotation pole. Hα, which appears consistently as emission in this star, shows dramatic variations in its equivalent width (by a factor of 4) and in its shape. Maximum Hα emission as well as very strong He I D_3 emission is seen at the phase when the high-latitude spot transits the disk, which indicates that chromospheric activity such as plage and flares may be associated with this spot feature.

Subject headings: line: profiles — stars: activity — stars: chromospheres — stars: individual (V410 Tauri) — stars: pre–main-sequence

1. INTRODUCTION

It is well accepted that starspots several hundred degrees cooler than the stellar photosphere are responsible for the photometric variations seen in a variety of active late-type stars such as RS CVn systems, FK Comae, and BY Dra stars. Many of these stars possess high rotational velocities making it possible to apply the Doppler imaging technique to derive the surface distribution of cool spots on these stars (e.g., Vogt, Penrod, & Hatzes 1987). This technique, in various forms, has been used to image photospheric spots on a number of active late-type stars (e.g., Vogt & Penrod 1983; Vogt & Hatzes 1991; Hatzes & Vogt 1992; Kürster et al. 1992; Strassmeier 1994) These images have revealed that large polar spots with appendages extending down to low latitudes are a common feature among active, rapidly rotating late-type stars. The spot distributions often show isolated equatorial spots and one hypothesis is that magnetic flux (believed to be traced by the cool spots) first emerges at the equator and then migrates toward the rotation pole (Vogt & Penrod 1982). Schüssler & Solanki (1992), on the other hand, have argued that for rapidly rotating stars the Coriolis force can dominate the buoyancy force causing magnetic flux to emerge near the rotation pole.

Doppler imaging studies of most stars have concentrated on RS CVn stars which are evolved objects whose large rotational velocities result from the tidal spin-up by a stellar companion. A few FK Comae stars have also been imaged (Vogt 1988; Piskunov, Tuominen, & Vilhu 1990; Kürster et al. 1992), but these stars are also evolved objects that are believed to be the end product of a coalesced binary. Doppler images of the spot distributions on other classes of objects, especially in different evolutionary states, may provide a better understanding of stellar activity as a function of stellar age, tidal effects, rotational velocity, and other parameters. T Tauri stars are a class of active stars that, unlike RS CVn and FK Comae stars, are pre–main-sequence objects. The large rotational velocities of these stars result from the conservation of angular momentum as the star contracts to the main sequence, thus the magnetic activity of these stars may be more closely related to the type of activity the Sun experienced at a very young age.

V410 is a T Tauri star with relatively weak Hα emission and very little infrared excess (Cohen 1974; Rydgren et al. 1984; Ruciński 1985a). This lack of "veiling" that is seen in most other T Tauri stars (e.g., Basri & Batalha 1990) suggests that it is a member of the post, or "naked" T Tauri stars (Walter 1987). This star also exhibits large (up to 1 mag in V) photometric variations (Rydgren & Vrba 1983; Vrba, Herbst, & Booth 1988) that are believed to be due to cool photospheric spots. V410 Tau's large rotational velocity ($\sim$70 km s^{-1}), relative brightness, and the fact that the photosphere may not be obscured by a stellar disk make this an ideal candidate for Doppler imaging.

Vrba et al. (1988) obtained 5.4 yr of UBVRI photometry for V410 Tau and found that a single period of 1.871 $\pm$ 0.0001 days could be applied to the entire span of observations, which indicates, perhaps, that the spot responsible for the photometric variations is long lived. The wavelength dependence of the light curve could be modeled by spots 1000–1400 K cooler than the photosphere and covering up to 43% of the surface. Herbst (1989) subsequently modeled 8 yr of photometry using two large (radius $> 40°$) spots; one located at high latitude ($> 50°$) and the other in the opposite hemisphere. He concluded that the changes in shape and amplitude of the light curve at different epochs resulted primarily from changes in the relative longitudes of the spots.

The first Doppler image of V410 Tau was presented by Strassmeier, Welty, & Rice (1994) using six nights of data taken in 1992 November at Kitt Peak National Observatory. That image was dominated by a large spot at high latitude ($l = 70°$) that did not straddle the rotation pole, unlike high-latitude features on RS CVn and FK Comae–type stars. They also claimed evidence for hot spots 500 K hotter than the photosphere. This high-latitude spot activity was also confirmed by Joncour, Bertout, & Ménard (1994b), who derived a Doppler image using data taken in 1990 January.

TABLE 1

V410 TAURI: OBSERVATIONS[a]

JD 2,440,000+	Phase	Exposure (minutes)	S/N
9321.692	0.84	60	140
9321.873	0.94	60	170
9322.715	0.39	60	170
9322.899	0.48	60	140
9357.631	0.05	70	140
9358.623	0.58	60	80
9405.669	0.72	70	140
9406.648	0.25	60	145
9407.654	0.78	60	200

[a] Ephemeris: 2,446,861.629 + 1.871E.

In this paper, the spot distribution on V410 Tau centered on epoch 1994.0 was derived using several photospheric lines and the Doppler imaging technique. The spectral observations show large variations in the Hα emission as well as two instances where He I D_3 appears in emission.

2. DATA ACQUISITION

Data were acquired on seven nights spanning 86 days in late 1993 and early 1994 using the Sandiford Echelle Spectrograph of the McDonald Observatory 2.1 m telescope and a Reticon 1200 × 400 CCD detector. The details of the instrument can be found in McCarthy et al. (1993). This prism crossed-dispersed echelle spectrometer, which is mounted at the Cassegrain focus of the 2.1 m telescope, provides large (up to 1500 Å) wavelength coverage at high resolution ($R \approx 60{,}000$). The spectrograph setup for the V410 Tau observations was chosen such that a wavelength coverage of ~5700–7100 Å was obtained. A 150 μm slit (1".5 subtended on the sky) projected to 3 pixels on the detector and resulted in a resolving power of ~40,000 (resolution = 0.18 Å at 6410 Å).

Observations were phased using the ephemeris of Vrba et al. (1988):

$$\text{JD } 2{,}446{,}861.629 + 1.871E$$

and are listed in Table 1 along with the Julian Day of the observations, the rotation phase, exposure times, and the signal-to-noise per resolution element.

Typical spectra acquired using this instrumental setup are presented in Figure 1. It shows, at two rotational phases, the spectral order containing Fe I λ6430 and Ca I λ6439, spectral lines traditionally used for Doppler imaging. Note the spectral distortions that appear in virtually all spectral lines, a signature of very cool starspots that contribute negligible amounts to the observed flux. At phase 0.78 (*top spectrum*), all the spectral lines are noticeably flat bottomed due to a spot feature near disk center. By phase 0.94 there is a strong asymmetry on the red side of each line, which indicates that the spot has already passed the disk center and is receding toward the stellar limb.

3. IMAGING PHOTOSPHERIC SPOT FEATURES

3.1. *Determination of Stellar Parameters*

The projected rotational velocity (v sin i) of V410 Tau has been measured by various investigators as 76 ± 10 (Vogel & Kuhi 1981), 70.9 ± 9 (Hartmann et al. 1986), and 75 km s^{-1} (Patterer et al. 1993). The v sin i was measured from the McDonald data using three spectral lines: Ca I λ6439, Fe I λ6430, and Fe I λ6400. In each case, the spectral distortions due to spot features were smeared by summing the individual lines over a complete rotation cycle. A rotationally broadened profile was calculated by integrating local specific intensity profiles across a stellar disk. These intensity profiles were generated using model atmospheres of Bell et al. (1976) and a stellar grid of 120 × 120 elements. The final synthetic profiles were then compared to the mean of the observed profiles. The three spectral lines resulted in a v sin i of 77 ± 1 km s^{-1}, consistent with previous determinations. The points in Figure 2 show the mean profile of Ca I λ6439 created by summing the nine observed rotation phases. The solid line represents a synthetic line having a v sin i of 77 km s^{-1}. Note that the mean spectral line has a shape close to that of a rotationally broadened profile. This is in sharp contrast to the mean profile shape seen in RS CVn–type stars that can be significantly flat bottomed (e.g., EI Eri; Hatzes & Vogt 1992).

The stellar inclination of V410 Tau is unknown. In modeling the photometry, Herbst (1989) concluded that the stellar inclination was $75° < i < 85°$. Although the gross features of the spot distribution derived using Doppler imaging are relatively

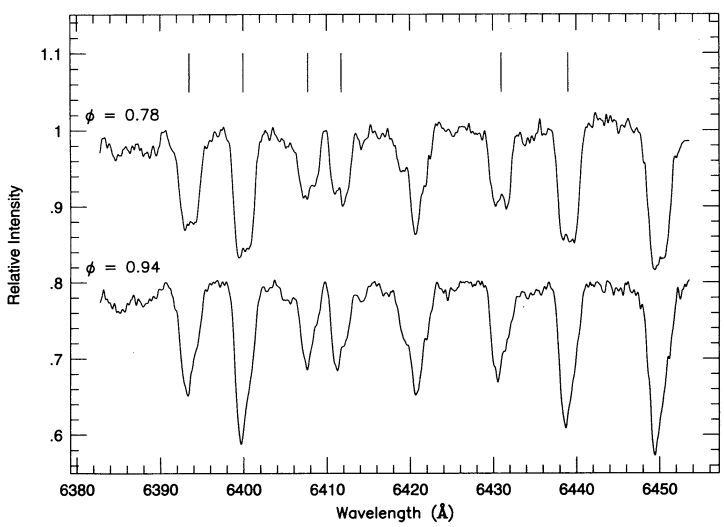

FIG. 1.—The spectral region 6382–6454 Å for V410 Tau at two rotation phases. The distortions visible in all unblended lines are due to cool photospheric spots. Vertical lines indicate those spectral lines used for Doppler imaging.

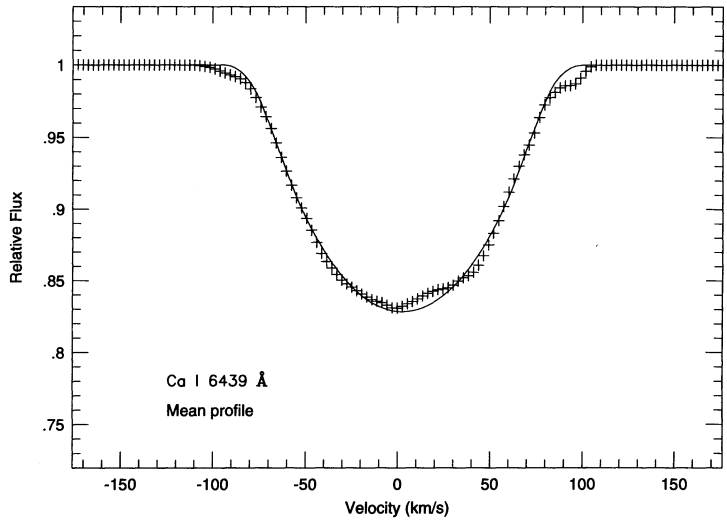

FIG. 2.—The mean Ca I λ6439 Å spectral line (*crosses*) computed by co-adding all the observations. The solid line represents a rotationally broadened profile having a $v \sin i$ of 77 km s^{-1}.

insensitive to assumptions about the inclination of the star (Vogt et al. 1987), it is possible to infer an inclination using this technique, but with relatively low accuracy ($\pm 10°$). Using test cases of known spot distributions, Hatzes, Penrod, & Vogt (1988) demonstrated that the final misfit (χ^2) between the observed spectral line profiles and the fits from the derived spot distribution was minimized whenever the proper stellar inclination was used. In other words, the best fit to the data is obtained when using the correct stellar inclination. Kürster, Schmitt, & Cutispoto (1994) applied a similar method to determine the inclination of AB Dor.

Doppler images were derived using the Ca I spectral line profiles and several values of the input inclinations. Figure 3 shows the χ^2 (normalized by the minimum value) for four values of the input inclination along with a line representing a parabolic fit with a minimum at 54°. This value was adopted as the stellar inclination for V410 Tau in all image reconstructions.

3.2. *Doppler Images*

Doppler images were derived using the maximum entropy method (MEM), the details of which can be found in Vogt et al. (1987). Only cool spots were allowed in the modeling, in spite of the fact that Strassmeier et al. (1994) claimed to have found evidence for hot spots on V410 Tau. There is a danger in using a totally unconstrained reconstruction (i.e., both hot and cool spots) in Doppler imaging without simultaneous photometry which can be used to establish the true continuum level. If the true continuum level is unknown, it is possible for the technique to use a combination of hot and cool spots to fit the line profiles even when only cool spots are present. (In fact, an unconstrained maximum entropy method prefers a combination of hot and cool spots). Thus the presence of hot spots in Doppler images may be artifacts. Since there was no photometry to accompany the spectral observations and the presence of cool starspots on V410 Tau is well established via

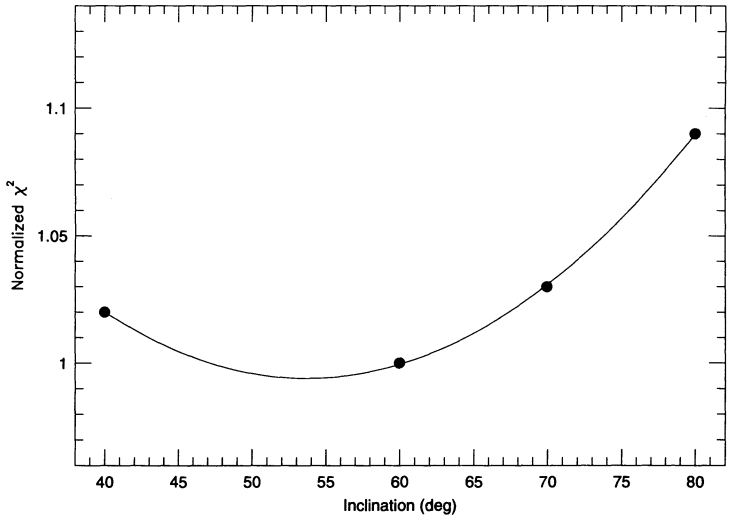

FIG. 3.—The measure of misfit (χ^2 normalized by the minimum value) between observed and model spectral lines as a function of stellar inclination angle used in the Doppler imaging reconstruction.

TABLE 2

SPECTRAL LINES USED FOR DOPPLER IMAGING

λ (Å)	Species	χ (e.v.)	EW (mÅ)
6393.6.....	Fe I	2.43	320
6400.0.....	Fe I	3.60	435
6408.0.....	Fe I	3.69	235
6411.7.....	Fe I	3.65	239
6430.9.....	Fe I	2.18	276
6439.1.....	Ca I	2.52	223

using the Ca I line at λ6439 and the Fe I lines λλ6430, 6339, photometry, the technique was constrained to find only spots cooler than the photosphere. This does not mean that hot spots actually do not exist on V410 Tau, just that the modeling procedure employed in this paper was biased toward finding spots cooler than the photosphere.

A total of six stellar spectral lines were used to derive five individual Doppler images. The data for V410 Tau were of much lower signal-to-noise than data typically acquired on Doppler imaging candidates. Furthermore, the $v \sin i$ of V410 Tau is rather high, and this results in shallower lines which exacerbates the low signal level. Use of several maps would help distinguish between the true features that should be present in all images and spurious features due to noise or line blending.

The spectral lines employed are listed in Table 2 and indicated by the vertical lines in Figure 1. Although the Sandiford Echelle Spectrograph simultaneously collects data on many lines, most of these are too severely blended to be useful for Doppler imaging. (Unfortunately, the Li I λ6707 line that was used by Joncour et al. [1994b] for their Doppler image was not obtained in the present study. The Sandiford is used in Littrow and the central two orders, one of which contained the lithium line, which was lost due to internal reflections.) The Fe I λλ6408, 6411 lines were of equal strength and much weaker than the other lines used for Doppler imaging. In order to decrease the noise level in the final map derived from these spectral lines, a reconstruction was made from the average profiles of the two lines. Specific intensity profiles used in the reconstruction process were generated using model atmospheres of Bell et al. (1976) and R. L. Kurucz's WIDTH5 routines.

Figures 4–8 show the resulting Doppler images derived 6400, and λλ6408 + 6411. These are shown as a gray scale in "pseudo-Mercator projection" (i.e., latitude vs. rotation phase). Darkest regions correspond to a temperature ~900 K below the photospheric value and the lightest shade of gray that is just visible corresponds to a temperature 300 K below the photosphere. The Doppler images show remarkable consistency with the dominant features reproduced in all maps. The slight differences between the maps are most likely due to noise in the data or possibly line blending. There appear to be no significant differences between the images derived from the stronger lines and those from the weaker lines.

The spectral line fits to Ca I λ6439 and Fe I λ6430 are shown in Figures 9 and 10, respectively. In both cases the data are represented by vertical bars indicating the uncertainties in the flux measurements and a line representing the line profile fits resulting from the Doppler images. The fits to the other observed line profiles are of comparable quality and to conserve space these were not shown.

The Fe I λ6430 line appears to have a moderate blend in the red wing. Such blends can be a serious problem when using the spectra of rapidly rotating stars. This coupled with the low signal-to-noise ratio of the V410 Tau data set makes it difficult to establish where the line-free regions of the spectrum are when normalizing the continuum. This may account for some of the apparent variations in the strength of this blend. (It is also possible that this blend arises from the spotted regions of the star.) No attempt was made to treat this blend in the modeling process. MEM primarily models changes in the spectral line shapes that are consistent with the rotational period of the star. Consequently blends, for the most part, are ignored by the reconstruction process. Furthermore, by averaging several images derived using separate lines should minimize the presence of artifacts that may be due to the presence of such blends.

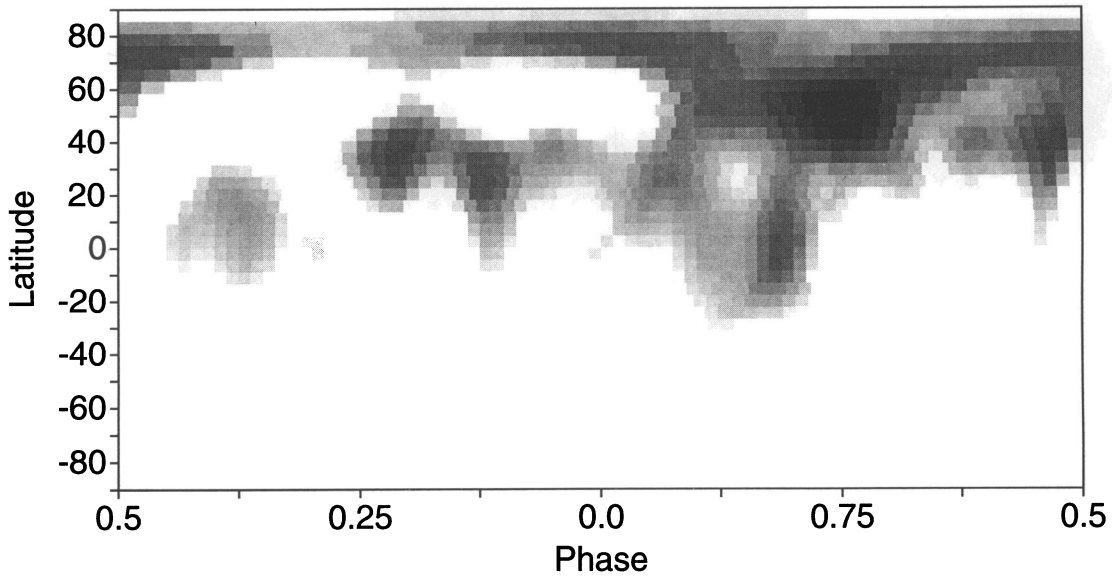

FIG. 4.—A gray scale of the Doppler image derived using the Ca I λ6439 shown in pseudo-Mercator projection. In all gray-scale maps, black regions represent a minimum pixel value of ~3200 K and white regions represent the photospheric value of 4400 K.

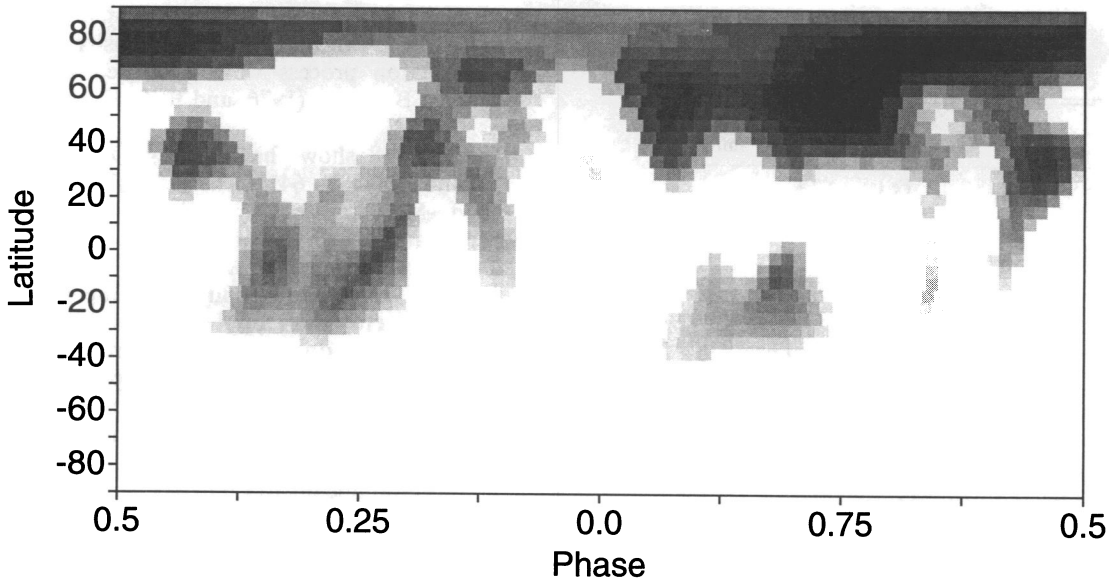

FIG. 5.—A gray scale of the Doppler image derived using the Fe I λ6430 in pseudo-Mercator projection

The individual Doppler images shown in Figures 4–8 were used to produce an average image. This mean image is displayed in three different projections so as to facilitate comparison to other published images. Figure 11 shows the mean Doppler image in pseudo-Mercator projection. This projection can be directly compared to the image derived by Strassmeier et al. (1994). This same image is shown in a flattened polar projection in Figure 12. In the latter projection latitude lines are drawn in equally spaced intervals down to a latitude of −30°. Each square represents an image pixel 4°.5 × 4°.5. The heavy line represents the stellar equator. The radial tic marks about the star indicate the observed phases. Finally, Figure 13 shows the mean Doppler image in a stereographic projection at four rotation phases ($\phi = 0.0$, 0.25, 0.5, and 0.75). In this instance, all image pixels with a temperature less than 500 K below that of the photospheric value are shown by crosses. (This "thresholded" image can be considered to be a fair two-temperature representation of the smooth MEM image.) This last projection can be compared directly to Figure 6 of Herbst (1989) or Figure 2 of Joncour et al. (1994b). In comparing the image of this work to other images of V410 Tau one can see that a high-latitude spot with similar shape and size has persisted on V410 Tau for several years.

The predicted V-light curve from the average Doppler image is shown in Figure 14. This was calculated using the mean Doppler images and without converting the smooth MEM image into a two-temperature distribution. MEM tends to smooth the transition from spot to photosphere, even if the true boundary is very sharp, and as a result the reconstructed spots may be warmer than they actually are. Consequently, the amplitude of this predicted light curve may be underestimated. This light curve should be taken as a qualitative rather than a

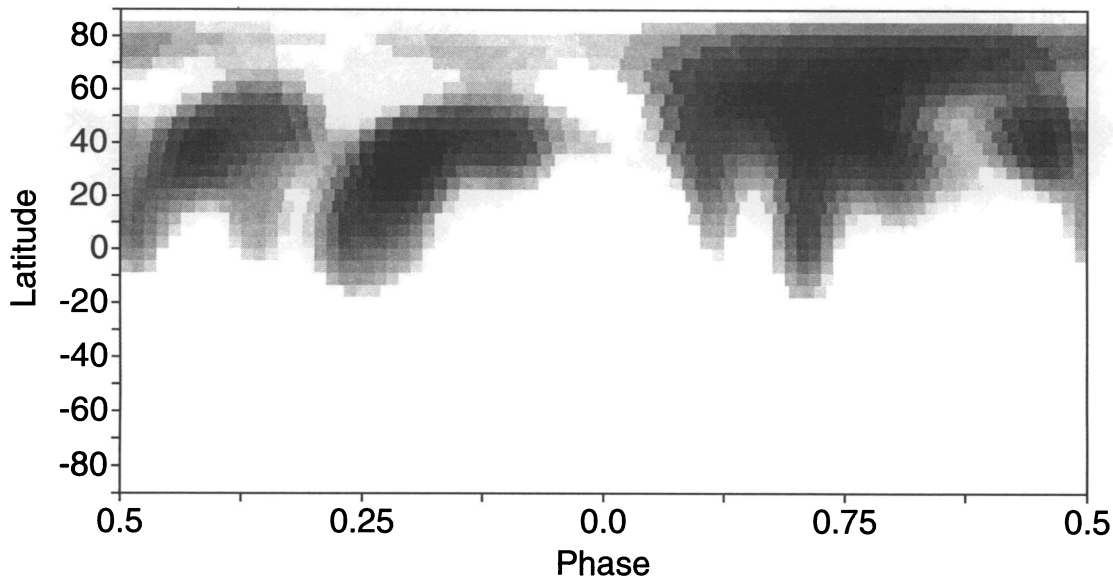

FIG. 6.—A gray scale of the Doppler image derived using the Fe I λ6393 in pseudo-Mercator projection

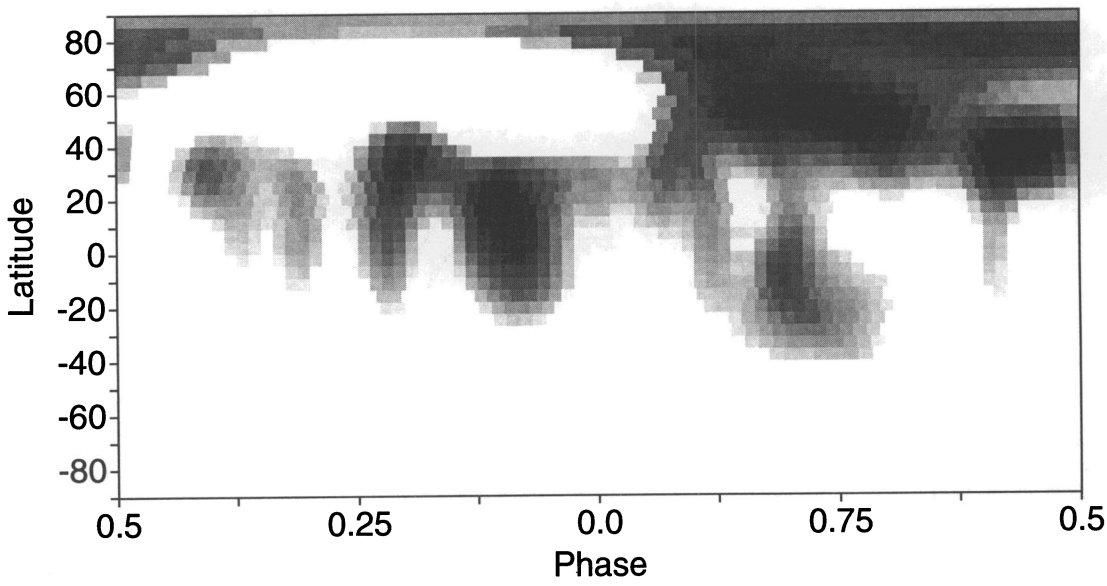

FIG. 7.—A gray scale of the Doppler image derived using the Fe I λ6400 in pseudo-Mercator projection

quantitative one since the shape of the curve is more accurate than the amplitude. The true amplitude is set by the actual spot area and temperature.

4. CHROMOSPHERIC ACTIVITY INDICATORS

4.1. Hα *Emission*

Figure 15 shows the Hα line profiles as a function of rotation phase. The Hα profile changes from almost no emission at phases 0.05 and 0.25 to very strong emission with broad, high-velocity wings (± 200 km s^{-1}) at phases 0.72 and 0.78. At times the Hα emission profile can have a strongly asymmetric shape (e.g., $\phi = 0.84$).

Figure 16 shows the emission equivalent width (EEW) of Hα above the continuum as a function of rotation phase. Data points are repeated for the second cycle to facilitate in discerning sinusoidal variations. These EEWs were corrected for the changes in the continuum level due to the spot distribution. The photometric *R*-curve (similar to the *V*-band curve in Fig. 14) used for these corrections was computed using the spot distribution shown in Figures 11 and 12. There appears to be rotational modulation of the emission with a maximum around phase 0.8. The data were accumulated over 3 months, so it is not clear whether this modulation is due to long-lived surface features such as plage or to transient events such as flares occurring at just a few phases. Interestingly, the peak of the Hα emission coincides with the phases when the high-latitude spot is best in view. If the emission is due to plage or a flare, then perhaps it is associated with this large polar spot.

The behavior of He I D_3 emission lends some support to the premise that flares may be responsible, in part, for some of the observed Hα emission. The He I feature appears as absorption

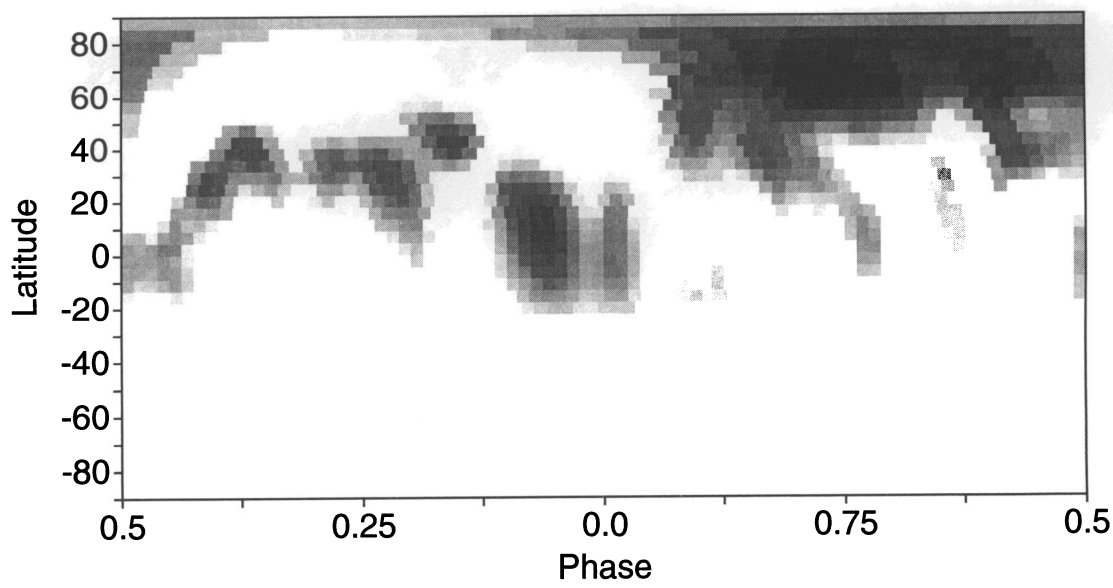

FIG. 8.—A gray scale of the Doppler image derived using the average of the Fe I λλ6408, 6411 lines, again in pseudo-Mercator projection

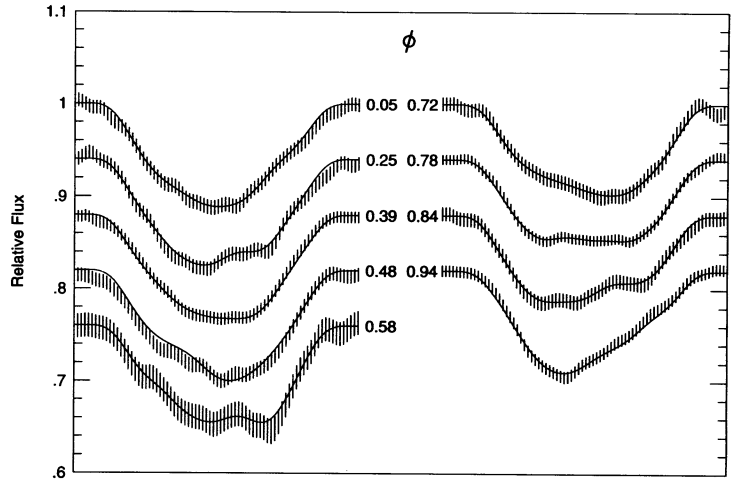

FIG. 9.—The observed Ca I λ6439 line flux profiles (*vertical bars*) and the fits (*lines*) produced from the Doppler image shown in Fig. 1. The length of each vertical bar represents the error in the flux measurement at that point.

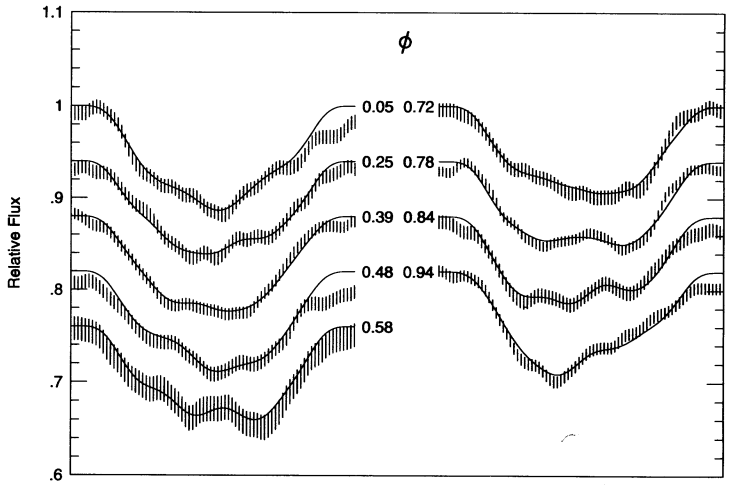

FIG. 10.—The observed flux profiles for the Fe I λ6430 (*vertical bars*) as well as the fits (*lines*) from the Doppler image

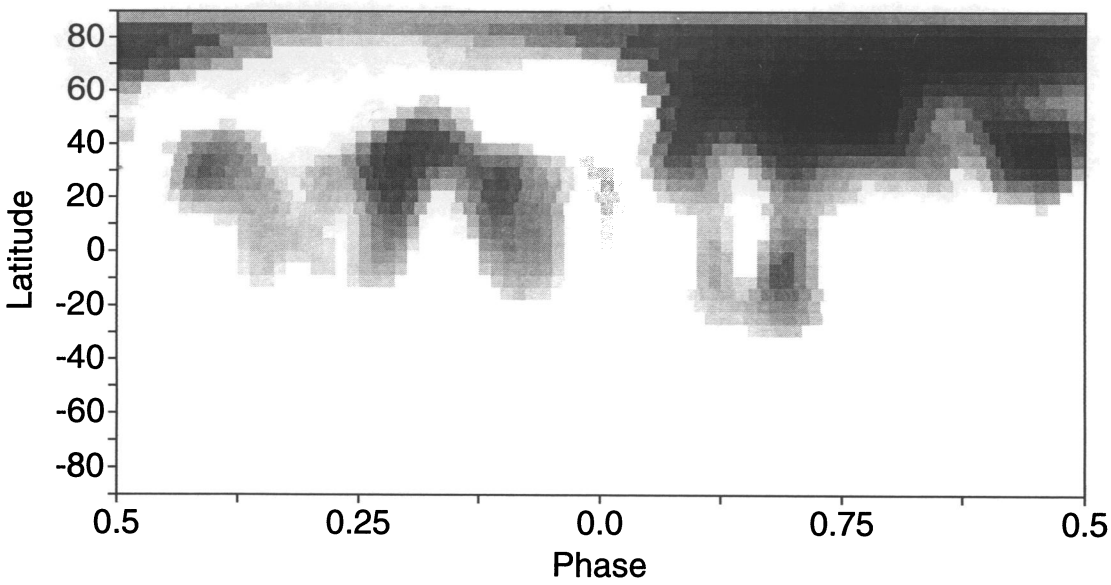

FIG. 11.—A gray scale of the average of the Doppler images presented in Figs. 4–8

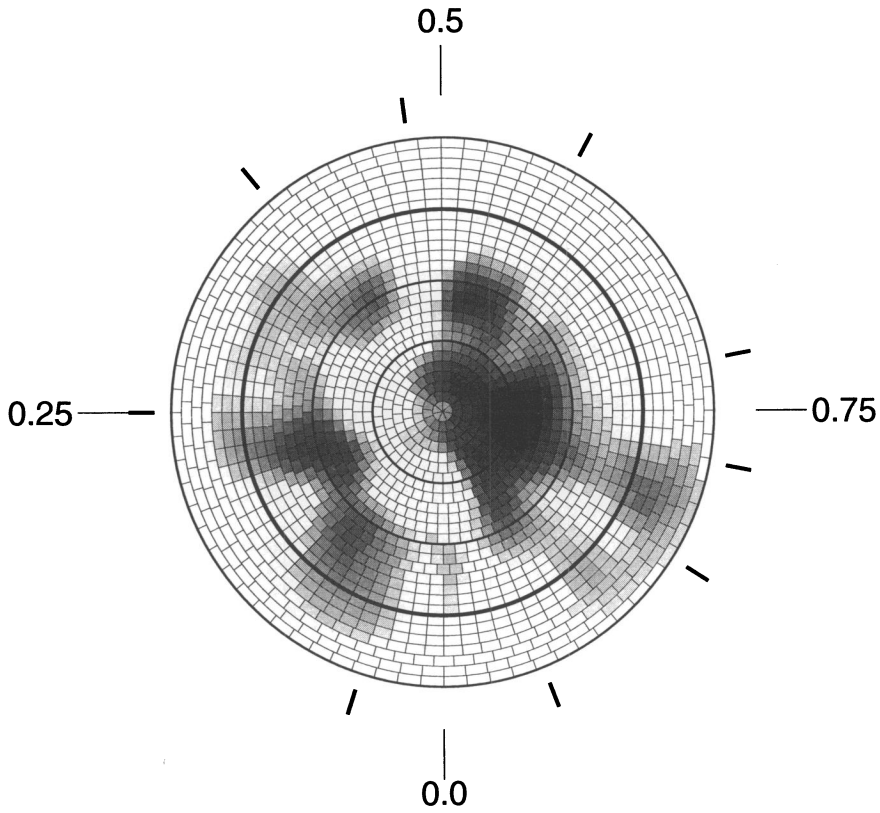

FIG. 12.—A flattened polar view of the average Doppler image (Fig. 11). Each square represents a 4°.5 × 4°.5 image pixel. The bold line represents the stellar equator and the radial tic marks around the star indicate the observed phases.

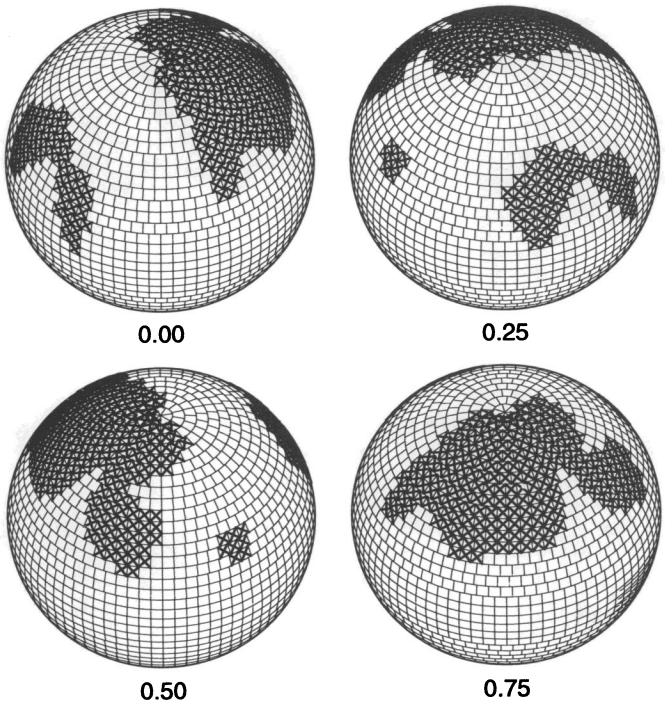

FIG. 13.—The average Doppler image of V410 Tau shown in stereographic projection at four rotation phases (ϕ = 0.0, 0.25, 0.50, and 0.75). All pixels with a temperature less than 500 K below the photospheric value are shown as spotted regions (*crosses*). All other image pixels are displayed as photosphere (*white*).

in plage or weak flares and as emission in strong flares (Zirin 1988). For most observed phases in V410 Tau, the spectral region near this feature does not appear strongly in either emission or absorption. Any weak absorption may be lost in the continuum due to the rapid rotation of this star. There are two instances when He I appears in emission. Figure 17 shows the "mean" spectral region around He I that was produced by averaging those observations that did not show any appreciable He I emission. The bottom spectrum, taken at phase 0.78, shows He I strongly in emission and redshifted by $\sim$20 km s^{-1}. Observations made 2 days prior to this at phase 0.72 did not show any emission near the He I line. The central panel shows a spectrum taken at phase 0.39 and 85 days prior to the spectrum at ϕ = 0.78. The level of He I emission is considerably lower than at ϕ = 0.78, but still noticeable. It also appears to be redshifted by $\sim$40 km s^{-1}.

5. DISCUSSION

The Doppler images of V410 Tau presented here confirm the presence of high-latitude spot activity shown in previous published images. The large spot on V410 Tau in 1994.0 appears to have the same shape and size as a feature seen in the Doppler images of this star from 1990 (Joncour et al. 1994b), 1992 (Strassmeier et al. 1994), as well as the spot distribution modeled from photometry taken in 1987 (Herbst 1989). The high-latitude spot on V410 Tau, like the polar spots on RS CVn–type star, seems to persist for many years. There does, however, appear to be a migration in longitude when phasing to the ephemeris of equation 1. In 1990 January this feature

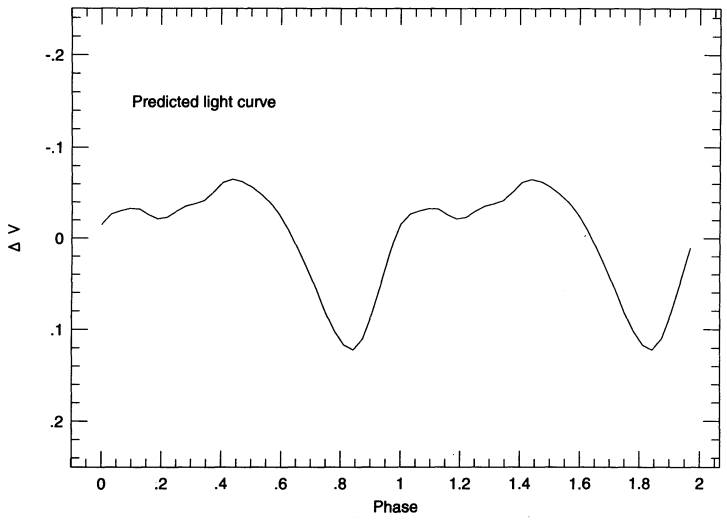

FIG. 14.—The predicted *V*-light curve calculated using the mean Doppler image (Fig. 11)

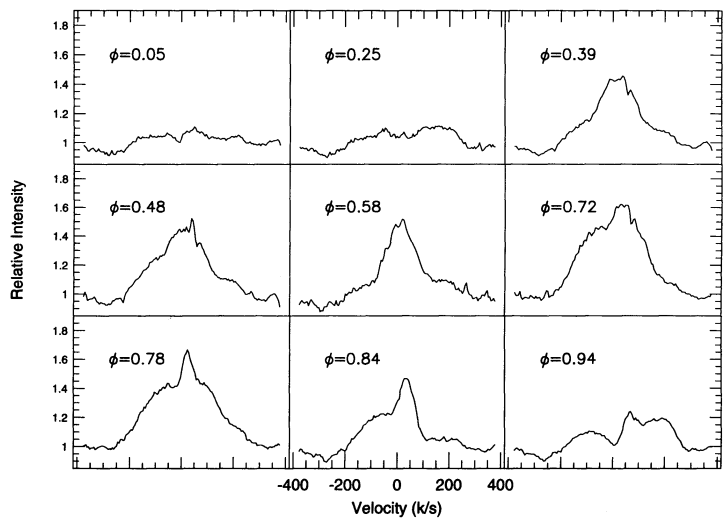

FIG. 15.—The Hα profiles of V410 Tau as a function of rotation phase

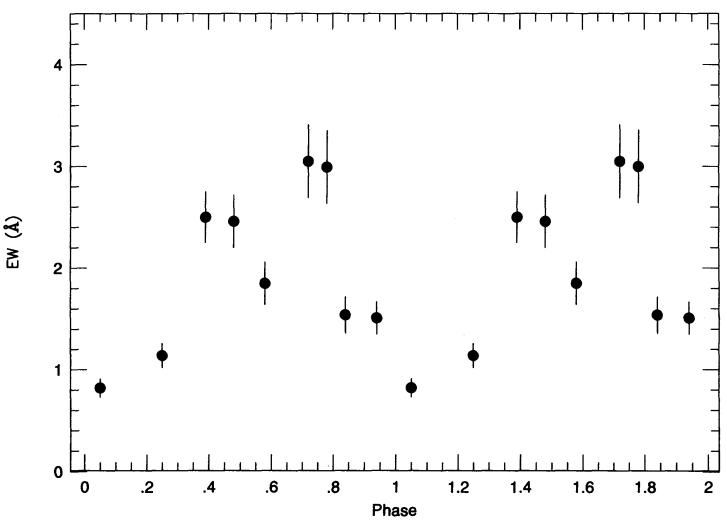

FIG. 16.—The Hα equivalent width (in angstroms) as a function of rotation phase. Values were corrected for the changes in continuum level due to the spot distribution using a predicted *R*-band light curve.

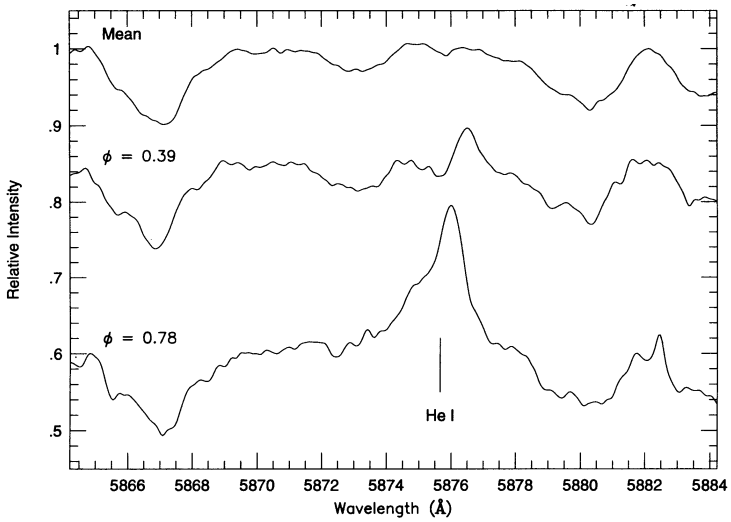

FIG. 17.—The spectral region around He I λ5876 for the averaged observations (excluding $\phi = 0.39$ and 0.78), along with observations at phases 0.39 and 0.78). The wavelength position of the He I D_3 line is indicated by the vertical line.

was centered on phase 0.11 and in 1992 November the high-latitude spot was centered on phase 0.45. The Doppler image presented here (Fig. 12) shows this feature centered on phase 0.75 in 1994.0. If this feature is indeed the same spot in all Doppler images then a natural explanation for the apparent migration is that the true period is slightly longer than that used in computing the phases. An $O-C$ diagram of the observed minus computed times for the transit of the large high-latitude spot yields a revised period that is ≈ 1.872 days. Herbst (1989) suggested a revised period of 1.8714 days based on an $O-C$ diagram for the minimum light of V410 Tau, although he was not completely sure of this result. The photometric $O-C$ diagram showed an almost linear trend from 1984 to 1989, but data prior to 1983 was inconsistent with this trend. More recently Petrov et al. (1994) analyzed 7 yr of photometry from 1986 to 1992 and found a period $P = 1.872095 \pm 0.000022$ days. This latter value is consistent with the period inferred from the Doppler images.

Further evidence for high-latitude magnetic activity seems to be provided by radio measurements. Bieging & Cohen (1989) measured the radio flux densities of V410 Tau at monthly intervals over a 1 yr period with the VLA and found evidence for modulation of the radio emission with a period of 0.933 days, or about half the optical period. They concluded that this could be explained by magnetic loop structures having one of two geometries: (1) two loops located at opposite hemispheres of the star or (2) a single loop located at high latitude and extending far enough above the pole of the star so as to always be in view. The latter geometry is consistent with the Doppler images presented here and by other investigators.

Hα emission attains its maximum strength near phase $\approx$0.7–0.8, coincident in time with the appearance of a strong emission feature near the wavelength location of He I D_3. Both of these may be due to flare activity, possibly associated with the high-latitude spot. Vrba et al. (1988) found that flares in the U band were seen primarily near minimum light or when the dominant spot (i.e., high-latitude feature) transits. Modest He I emission that is strongly redshifted ($\approx$40 km s^{-1}) also appears at one observation at phase 0.39, coincident with the passage of a small low-latitude spot. The large redshift could result either from mass motions resulting from a flare event over the small low-latitude spot at disk center or from the rotational Doppler shift of the star if the flare occurred at low latitude near the limb. The fact that the He I emission was seen in two out of nine observations suggests that the rate of flaring on V410 Tau may be rather high.

The v sin i measurement for V410 Tau together with the inclination inferred from the Doppler imaging, and the rotation period implies a stellar radius of 3.46 $R_\odot$, considerably larger than the 2.46 $R_\odot$ calculated by Herbst (1989). His calculation used a much lower value of the v sin i as well as a higher estimate for the stellar inclination. A calculation of the luminosity and effective temperature similar to the one performed by Herbst (1989), but using the larger radius resulted in $L = 3.16\ L_\odot$ and $T_{\rm eff} = 4100$ K. This calculation assumed a distance of 160 pc to the Taurus cloud of which V410 Tau is a member (see Herbst 1989). These values place V410 Tau near the evolutionary track of a 1 $M_\odot$ star with an age of 300,000 yr (see theoretical H-R diagram in Strom et al. 1989), as opposed to the 10^6 yr estimate of Herbst (1989). This age estimate can be made more consistent with Herbst's value if the star had a much higher inclination ($\approx$90°) or higher effective temperature (4400 K). However, the higher effective temperature would also imply a greater distance to the Taurus cloud by a factor of 1.5.

It is intriguing that the high-latitude spot seen on V410 Tau is not centered on the rotation pole as are similar features on RS CVn stars. In many respects this feature on V410 Tau has more similarities to the "polar" spots on other young, pre–main-sequence stars. Doppler images of V824 Ara (Kürster et al. 1992) showed a decentered polar spot very similar to that of V410 Tau. AB Dor showed a high-latitude spot only in epoch 1987.9 (Kürster et al. 1992; Kürster & Dennerl 1993). At other epochs (1989.1, 1990.8, and 1991.9) AB Dor showed spots concentrated in an active latitude of $\approx +25°$ and no polar feature (Kürster et al. 1992). Joncour, Bertout, & Bouvier (1994a) recently published a Doppler image for the weak T Tauri star HDE 283572 which showed one large polar spot. All these stars are believed to be young, pre–main-sequence objects. Strassmeier et al. (1994) suggested that the presence of a polar spot may be due to a combination of stellar age and the time within its activity cycle that the star is observed. AB Dor has an estimated age of 10^6–3×10^7 (Ruciński 1982, 1985b; Vilhu,

Gustafsson, & Edvardsson 1987), which makes it older than V410 Tau. Perhaps this star has a spot morphology that is changing from one dominated by a high-latitude feature such as V410 Tau to one dominated by an active latitude band as is the case for the Sun. However, the spot morphology depends in a complicated manner on stellar age, rotation rate, depth of convection zone, etc., so that monitoring the spot activity on other pre–main-sequence stars having a variety of stellar ages and rotation rates are needed to discern what stellar parameters influence spot morphology.

The fact that the Doppler imaging technique as applied to V410 Tau does not produce a centered polar cap as is often seen in the images of RS CVn stars provides strong indirect evidence that these features on other active stars are in fact real. It has often been criticized that the polar spot feature on RS CVn stars is either an artifact of the technique or of a poor understanding of the atmospheric parameters of the stars. If these features were an artifact of the technique, then a centered polar spot should have been seen on V410 Tau, and this is not the case.

This research was supported by NSF grant AST-91 16478. The author wishes to thank M. Kürster for useful discussions and for his critical reading of the manuscript.

REFERENCES

Basri, G., & Batalha, C. 1990, ApJ, 363, 654
Bell, R. A., Eriksson, K., Gustafsson, B., & Nordlund, Å. 1976, A&AS, 23, 37
Bieging, J. H., & Cohen, M. 1994, AJ, 98, 1686
Cohen, M. 1974, MNRAS, 169, 257
Hartman, L., Hewett, R., Stahler, S., & Mathieu, R. 1986, ApJ, 309, 275
Hatzes, A. P., Penrod, G. D., & Vogt, S. S. 1989, ApJ, 341, 456
Hatzes, A. P., & Vogt, S. S. 1992, MNRAS, 258, 387
Herbst, W. 1989, AJ, 98, 2268
Joncour, I., Bertout, C., & Bouvier, J. 1994a, A&A, 291, L19
Joncour, I., Bertout, C., & Ménard, F. 1994b, A&A, 285, L25
Kürster, M., & Dennerl, K. 1993, in Physics of Solar and Stellar Coronae, ed. J. Linsky & S. Serio (Dordrecht: Kluwer), 443
Kürster, M., Hatzes, A. P., Pallavicini, R., & Randich, S. 1992, in ASP Conf. Ser., Vol. 26, Proc. 7th Cambridge Workshop on Cool Stars, Stellar Systems, and the Sun, ed. M. Giampapa & J. Bookbinder (San Francisco: ASP), 249
Kürster, M., Schmitt, J. H. M. M., & Cutispoto, G. 1994, A&A, 289, 899
McCarthy, J., Sandiford, B., Boyd, D., & Booth, J. 1993, PASP, 105, 881
Patterer, R. J., Ramsey, L., Huenemoerder, D. P., & Welty, A. D. 1993, AJ, 105, 1519
Petrov, P. P., Shcherbakov, V. A., Berdugina, S. V., Shevchenkom, V. S., Grankin, K. N., & Melnikov, S. Y. 1994, A&AS, 107, 9
Piskunov, N. E., Tuominen, I., & Vilhu, O. 1990, A&A, 230, 363.
Ruciński, S. M. 1982, Inf. Bull. Var. Stars, No. 2203
———. 1985a, AJ, 90, 2321
Ruciński, S. M. 1985b, MNRAS, 215, 591
Rydgren, A. E., Schmelz, J. T., Zak, D. S., & Vrba, F. J. 1984, Publ. US Naval Obs. Ser. 2, 25, Pt. 1, 1
Rydgren, A. E., & Vrba, F. J. 1983, ApJ, 267, 191
Schüssler, M., & Solanski, S. K. 1992, A&A, 264, L13
Strassmeier, K. G. 1994, A&A, 281, 395
Strassmeier, K. G., Welty, A. D., & Rice, J. B. 1994, A&A, L17
Strom, K. M., Strom, S. E., Edwards, S., Cabrit, S., & Skrutskie, M. F. 1989, ApJ, 97, 1451.
Vilhu, O., Gustafsson, B., & Edvardsson, B. 1987, ApJ, 320, 850
Vogel, S. N., & Kuhi, L. V. 1981, ApJ, 245, 960
Vogt, S. S. 1988, in IAU Symp. 132, The Impact of Very High S/N Spectroscopy on Stellar Physics, ed. G. Cayrel de Strobel & M. Spite (Dordrecht: Kluwer), 253
Vogt, S. S., & Hatzes, A. P. 1991, in IAU Colloq. 130, The Sun and Cool Stars: Activity, Magnetism, and Dynamos, ed. I. Tuominen, D. Moss, & G. Rüdiger (Berlin, Heidelberg; Springer), 297
Vogt, S. S., & Penrod, G. D. 1983, PASP, 95, 565
Vogt, S. S., Penrod, G. D., & Hatzes, A. P. 1987, 321, 496
Vrba, F. J., Herbst, W., & Booth, J. F. 1988, ApJ, 96, 1032
Walter, F. M. 1987, PASP, 99, 31
Zirin, H. 1988, in Astrophysics of the Sun (Cambridge: Cambridge Univ. Press)